International Journal of Biological Macromolecules 260 (2024) 129493

Contents lists available at ScienceDirect

International Journal of Biological Macromolecules

journal homepage: www.elsevier.com/locate/ijbiomac

Unveiling the mechanism of bactericidal activity of a cecropin A-fused endolysin LNT113

Jeongik Cho [a], Hye-Won Hong [b], Kyungah Park [a], Heejoon Myung [b,c], Hyunjin Yoon [a,d,*]

[a] Department of Molecular Science and Technology, Ajou University, Suwon, South Korea
[b] LyseNTech Co., Ltd., Seongnam, South Korea
[c] Department of Bioscience and Biotechnology, Hankuk University of Foreign Studies, Yongin, South Korea
[d] Department of Applied Chemistry and Biological Engineering, Ajou University, Suwon, South Korea

ARTICLE INFO

Keywords:
Gram-negative bacteria
Endolysin
Antimicrobial peptide
Lipopolysaccharide
Membrane permeability

ABSTRACT

Endolysins are lytic enzymes produced by bacteriophages at the end of their lytic cycle and degrade the peptidoglycan layer of the bacterial cell wall. Thus, they have been extensively explored as a promising antibacterial agent to replace or supplement current antibiotics. Gram-negative bacteria, however, are prone to resist exogenous endolysins owing to their protective outer membrane. We previously engineered endolysin EC340, encoded by the *Escherichia coli* phage PBEC131, by substituting its seven amino acids and fusing an antimicrobial peptide cecropin A at its N-terminus. The engineered endolysin LNT113 exerted superior activity to its intrinsic form. This study investigated how cecropin A fusion facilitated the bactericidal activity of LNT113 toward Gram-negative bacteria. Cecropin A of LNT113 markedly increased the interaction with lipopolysaccharides, while the *E. coli* defective in the core oligosaccharide was less susceptible to endolysins, implicating the interaction between the core oligosaccharide and endolysins. In fact, *E. coli* with compromised lipid A construction was more vulnerable to LNT113 treatment, suggesting that the integrity of the lipid A layer was important to resist the internalization of LNT113 across the outer membrane. Cecropin A fusion further accelerated the inner membrane destabilization, thereby enabling LNT113 to deconstruct it promptly. Owing to the increased membrane permeability, LNT113 could inactivate some Gram-positive bacteria as well. This study demonstrates that cecropin A fusion is a feasible method to improve the membrane permeability of endolysins in both Gram-negative and Gram-positive bacteria.

1. Introduction

The overuse and misuse of antibiotics have caused the emergence of multidrug-resistant bacteria (MDR). An increase in drug-resistant bacterial infections poses a serious threat to global health. Hence, there is an urgent need to develop novel antibiotics or other effective alternatives to battle MDR and overcome bacterial resistance. Bacteriophage-derived enzymes such as endolysins provide a promising solution to combat MDR. Phages utilize endolysins to disrupt bacterial peptidoglycan layers at the end of their replication cycle. Endolysins exert selective activity against target bacteria in contrast to conventional antibiotics, which have a broad-spectrum. Indiscriminate disturbance of the commensal microbiota has been a downside of broad-spectrum antibiotics [1]. Endolysins can be grouped into at least five classes of distinct enzymatic activities: *N*-acetyl-β-D-muramidases and *N*-acetyl-β-D-glucosaminidases break down the polysaccharide backbone of peptidoglycan layer but *N*-acetyl-β-D-muramidases cleave glycosidic bonds between *N*-acetylmuramic acid (MurNAc) and *N*-acetylglucosamine (GlcNAc), while *N*-acetyl-β-D-glucosaminidases hydrolyze bonds between GlcNAc and MurNAc, instead; lytic transglycosylases also cleave β-1,4 bonds between MurNAc and GlcNAc but do not require a water molecule for their catalytic activity; *N*-acetylmuramoyl-L-alanine amidases hydrolyze the amide bond between MurNAc and the peptide moiety; and lastly, endopeptidases hydrolyze peptide bonds between two amino acids in the peptide stem

Abbreviations: CBD, cell wall-binding domain; EAD, enzymatically active domain; GlcNAc, *N*-acetylglucosamine; IM, inner membrane; LAL, Limulus amoebocyte lysate; LB, Luria-Bertani; LPS, lipopolysaccharide; MDR, multidrug-resistant bacteria; MurNAc, *N*-acetylmuramic acid; OM, outer membrane; ONPG, *o*-nitrophenyl-β-D-galactopyranoside; PBS, phosphate-buffered saline; PCR, polymerase chain reaction; PI, propidium iodide; PVDF, polyvinylidene difluoride; SDS-PAGE, sodium dodecyl sulfate-polyacrylamide gel electrophoresis.

* Corresponding author at: Department of Applied Chemistry and Biological Engineering, Ajou University, Suwon 16499, South Korea.
E-mail address: yoonh@ajou.ac.kr (H. Yoon).

https://doi.org/10.1016/j.ijbiomac.2024.129493
Received 12 September 2023; Received in revised form 27 December 2023; Accepted 12 January 2024
Available online 13 January 2024

or in the cross-bridge that links the stems [2]. Because of the structural conservation of the peptidoglycan layers across bacterial genera or species, endolysins have a potential use as an alternative to antibiotics, lowering the chance of resistance development.

Currently, endolysins are being extensively investigated for therapeutic trials in Gram-positive bacterial infections [3]. However, they are obstructed when applied externally against Gram-negative pathogens. The outer membrane (OM), which is the outermost layer of Gram-negative bacteria, hinders endolysins from reaching the peptidoglycan layers beneath. Some exceptional endolysins with intrinsic activity against Gram-negative bacteria possess small globular structures with a molecular mass between 15 and 20 kDa, and are mostly composed of a simple module with only one enzymatically active domain (EAD), while lacking a cell wall-binding domain (CBD) [4,5]. Considering that phages infecting Gram-positive bacteria exploit the CBD of endolysins to anchor off post-lytic cell-wall remnants and limit lysis of the neighboring host cells [6], phages confined to Gram-negative bacteria are more likely to tune their endolysins for a better catalytic activity because the access of endolysins to the peptidoglycan of uninfected host cells is restrained by the OM, independent of the presence of CBD [7]. Moreover, the N- or C-termini of these exceptional endolysins, which exert natural lytic activity against Gram-negative bacteria, are mainly composed of positively-charged or hydrophobic amino acids, or amphipathic regions [8,9]. The lipopolysaccharide (LPS) layer in the outer leaflet of the OM is composed of three structural components, namely the outermost O-antigen, core oligosaccharide, and lipid A moiety and has the polyanionic nature attributable to phosphate groups of the core oligosaccharide and lipid A. The architectural configurations of these exceptional endolysins are proposed to facilitate their interaction with negatively-charged LPS and subsequent penetration across the OM of Gram-negative bacteria [10–12].

The structural characteristics of natural endolysins with catalytic activity against Gram-negative bacteria provide a clue to resolve the restriction of exogenous endolysins against Gram-negative pathogens. To increase the permeability of endolysins across the OM, various natural and synthetic membrane-disrupting peptides with cationic, hydrophobic, or amphipathic properties are fused to the parental endolysin proteins. Artilysins are representative endolysin hybrids containing OM-destabilizing peptides with polycationic, hydrophobic, or amphipathic properties, which enhance the binding affinity to LPS and their ability to diffuse across the OM [13]. Recently, we observed that an engineered endolysin LNT113 possessing cecropin A at its N-terminus exhibited superior killing activity against Gram-negative bacteria to its parental constructs of EC340 and mtEC340 [14]. EC340 is an endolysin from the *Escherichia coli* phage PBEC131, and its seven amino acids predicted at the EAD were substituted to improve its catalytic activity, resulting in mtEC340. Cecropin A (NCBI PRF 0708214A) is a natural antimicrobial peptide produced by the cecropia moth, *Hyalophora cecropia*, as a defense mechanism against bacterial infection. Structural studies suggest that the 37-residue polypeptide cecropin A is unstructured in aqueous phase but has the potential to fold into cationic α-helical conformation, which enables efficient interaction with biological membranes [15,16]. Although its bactericidal mechanism is unclear, cecropin-like peptides are proposed to form transmembrane pores or a carpet-like layer, rendering the membrane permeable [17,18]. In this study, we defined how cecropin A fusion facilitated the bactericidal activity of LNT113 against Gram-negative bacteria.

2. Material and methods

2.1. Bacterial strains and growth conditions

Bacterial strains used in this study and their growth conditions are listed in Supplementary Table 1. All strains were cultivated at 37 °C. *E. coli* strains defective in LPS, i.e., Δ*rfaC*, Δ*rfaL*, and Δ*lpxM*, were constructed using *E. coli* K-12 MG1655 as a parent strain through the λ Red recombination system [19]. In brief, the Kan^R cassette and flanking flippase recombinase target (FRT) sites of pKD13 were amplified using primers containing sequences homologous to the target genes. Polymerase chain reaction (PCR) products were introduced into *E. coli* harboring pKD46, and the recombinants selected on kanamycin plates were verified using PCR with diagnostic primers. All primers are listed in Supplementary Table 2. The Kan^R cassette was removed using a helper plasmid pCP20 encoding the flippase (FLP) recombinase. Ampicillin or kanamycin was added at 50 μg/mL when required. *E. coli* MG1655 intrinsically lacks O-antigen because of the disruption of the *wbbL* gene encoding the rhamnosyl transferase [20]. The *rfaL* (or *waaL*) gene encodes O-antigen ligase and therefore its absence is less likely to cause a detectable morphological phenotype in *E. coli* MG1655 [21]. A mutant strain devoid of *rfaC* (or *waaC*) fails to transfer heptose to the LPS core, and its core oligosaccharide lacks all (phosphorylated) sugars above the Kdo layer [22]. The *lpxM* (or *waaN*) gene encodes a myristoyl transferase that catalyzes the final step in lipid A biosynthesis, and its absence reduces acylation in the lipid A molecule [23].

2.2. Expression and purification of endolysins

Plasmids producing mtEC340 and LNT113 were introduced into *E. coli* BL21(DE3) star strain and induced for overexpression of recombinant endolysins, as described previously [14]. Briefly, bacterial cells at the logarithmic growth phase were treated with 0.5 mM isopropyl β-D-1-thiogalactopyranoside (Sigma-Aldrich, St. Louis, MO, USA) for 4 h at 25 °C and resuspended in lysis buffer (20 mM Tris-HCl, pH 7.5, 300 mM NaCl, and 20 mM imidazole) containing 1 mg/mL egg white lysozyme (Sigma-Aldrich) for 30 min. Cells were disrupted using sonication, and bacterial debris were removed using centrifugation at 10,000 ×*g* for 20 min at 4 °C. The supernatant was filtered through a 0.2 μm membrane, and the proteins were purified using Ni-NTA His-tag affinity chromatography. The eluted proteins were dialyzed in the storage buffer (20 mM Tris-HCl, pH 7.5, and 150 mM NaCl), and their concentration was measured using the Bradford assay (Bio-Rad, Hercules, CA, USA).

2.3. Mass spectrometry

Ion mobility mass spectrometry was performed on a SYNAPT XS instrument (Waters, Hertfordshire, UK) in Protium Science (Seongnam, Korea). LNT113 (25 μg) was loaded on a C4 column (Waters, ACQUITY UPLC BEH C4, 1.7 μm, 2.1 × 100 mm) and processed through UPLC system (Waters, ACQUITY Premier System) using a gradient of two types of mobile phases (buffer A: 0.1 % formic acid in deionized water, buffer B: 0.1 % formic acid in acetonitrile) at a rate of 0.3 mL/min for 15 min. LNT113 under reduced and non-reduced conditions were analyzed separately, as disulfide bonds may exert a role in protein structure. Under the reducing condition, LNT113 was treated with dithiothreitol at 10 mM for 15 min. MassLynx V4.2 SCN982 software (Waters) was used to analyze the spectra and calculate molecular masses and their mass errors.

2.4. Bacterial viability and turbidity reduction assay

Bacterial cells of *E. coli* O157:H7 EDL933 (ATCC 700927) or *E. coli* K-12 MG1655 at the mid-logarithmic growth phase were centrifuged at 10,000 ×*g* for 5 min, resuspended in 20 mM Tris-HCl (pH 7.5) buffer at approximately 10^6 cells/mL, and treated with 2 μM endolysins at 37 °C for 2 h. Following serial dilution in phosphate-buffered saline (PBS), the cell suspension was plated onto Luria-Bertani (LB) agar plates, after which the number of live cells was counted. For turbidity reduction assay, bacterial cells (approximately 10^8 cells/mL) were treated with endolysins at 1 and 2 μM, and optical density at 600 nm was measured using a Synergy HTX microplate reader (BioTek, Paramus, NJ, USA). As negative controls, equivalent numbers of bacterial cells were treated with 0 μM endolysin in both assays.

In turbidity reduction assay with other bacterial species, bacterial cells at approximately 10^8 cells/mL were resuspended in 20 mM Tris-HCl (pH 7.5) buffer and treated with LNT113 at 0.64 μM. Optical density after 1 h incubation was measured at 600 nm using a Synergy HTX microplate reader.

2.5. Minimum Inhibitory Concentration (MIC) measurement

The MIC was determined through the broth microdilution method using round-bottomed 96-well microtiter plates according to the guidelines of Clinical and Laboratory Standards Institute (CLSI). Bacterial cells under the mid-logarithmic growth phase were added in CAA media (5 g/L casamino acids, 5.2 mM K_2HPO_4, and 1 mM $MgSO_4$) at 10^6 cells/mL and treated with endolysins (1 to 64 μg/mL) at 37 °C for 20 h. The MIC was determined as the lowest concentration of an endolysin that inhibited the visible growth of test bacteria after 20 h incubation.

2.6. Confocal microscopy

Endolysins were conjugated with FITC using the FluoroTag™ FITC Conjugation Kit (Sigma-Aldrich). The FITC-conjugated endolysins were eluted with PBS in a column prepacked with Sephadex G-25M. *E. coli* MG1655 cells (approximately 1×10^8 cells) at the log growth phase were incubated with 5 μM FITC-conjugated endolysins and fixed in 4 % formaldehyde solution. Samples were placed on a slide glass and treated with Anti-Fade Fluorescence Mounting Medium (Abcam, Cambridge, UK) overnight. The images were obtained using a confocal microscope (A1R HD25 N-SIM S; Nikon, Tokyo, Japan) under a 100X oil immersion objective.

2.7. Limulus amoebocyte lysate (LAL) assay

LPS neutralization ability was measured using the Pierce™ Chromogenic Endotoxin Quant Kit (Thermo Fisher Scientific, Waltham, MA, USA), according to the manufacturer's instructions. Different concentrations of endolysins were incubated with 3.0 EU/mL *E. coli* O111:B4 LPS at 37 °C for 1 h and mixed with 50 μL of LAL reagent for 10 min. Substrate solution (100 μL) containing Ac-Ile-Glu-Ala-Arg-pNA was added and further incubated for 6 min. The coagulation cascade consists of a series of serine proteases, which get activated by proteolytic cleavage and then activate the subsequent protease. LPS triggers the activation of factor C, which in turn activates factor B and pro-clotting enzyme in sequence. The activated clotting enzyme catalyzes the release of yellowish *p*-nitroaniline (pNA) from Ac-Ile-Glu-Ala-Arg-pNA. As LPS neutralized by endolysin failed to activate the coagulation cascade, the level of unbound LPS was estimated by measuring the absorbance of pNA at 405 nm.

2.8. Isothermal titration calorimetry (ITC)

ITC experiment was conducted with MicroCal Auto-iTC200 calorimeter (Malvern Panalytical, Malvern, UK) at 25 °C at Korea Basic Science Institute (Ochang, Korea). LPS (0.5 mM) was loaded in a 40 μL syringe and an aliquot of 2 μL was injected into a 200 μL cell containing LNT113 or mtEC340 at 50 μM every 2.5 min. Endolysins and LPS from *E. coli* O111:B4 (Sigma-Aldrich, L2630, average M.W. 75 kDa) were prepared in HEPES buffer (pH 7.0, Sigma-Aldrich). The data were analyzed using MicroCal Origin software package (GE Healthcare, Chicago, IL, USA).

2.9. LPS extraction and analysis

LPSs of *E. coli* MG1655 and its mutants (Δ*rfaC*, Δ*rfaL*, and Δ*lpxM*) were extracted using a hot phenol-water micro-extraction method [24]. Bacterial cells resuspended in ddH_2O were mixed with pre-heated phenol solution at a 1:1 ratio and incubated at 68 °C for 15 min with vigorous vortexing every 5 min. After chilling on ice for 5 min, the phenol-water phases were separated via centrifugation at 10,000 ×*g* for 5 min. The aqueous phase containing LPSs was pooled and mixed with NaOAc (0.5 M) and 10 volumes of 95 % ethanol. After incubation at −20 °C overnight, LPSs were pelleted via centrifugation at 10,000 ×*g* for 5 min, re-dissolved in 100 μL ddH_2O, and precipitated again using 95 % ethanol. Finally, LPSs were dissolved in 50 μL ddH_2O and stored at −20 °C. The extracted LPSs were analyzed using sodium dodecyl sulfate-polyacrylamide gel electrophoresis (SDS-PAGE) using 15 % acrylamide gels. The gels were fluorescently stained using the Pro-Q® Emerald 300 Lipopolysaccharide Gel Stain Kit (Molecular Probes, Eugene, OR, USA), and LPSs were visualized using a ChemiDoc MP imaging system (Bio-Rad).

2.10. SYTO 9/propidium iodide (PI) staining

Bacterial cells at the log growth phase were resuspended in PBS at approximately 1×10^6 cells/mL and treated with 0.02 μM endolysins for 30 min. Bacterial cells were stained with 7.5 μM SYTO 9 (Invitrogen, Waltham, MA, USA) and 30 μM PI (Sigma-Aldrich), respectively, and incubated at 20 °C for 5 min in the dark. The stained cells were spotted onto 2 % (w/v) agar pads and observed with the EVOS® FL Imaging System (Life Technologies, Carlsbad, CA, USA). To measure the level of bacterial membrane disruption, bacterial cells resuspended in Tris-HCl buffer (pH 7.5) at approximately 10^8 cells/mL were treated with different concentrations (from 0 to 0.64 μM) of endolysins for 1 h and stained with 2 μM PI for 5 min. The fluorescence intensity of PI was recorded using Cycation 3 (BioTek) at λex 530 nm and λem 620 nm.

2.11. Membrane permeability test using β-lactamase and β-galactosidase assay

The *E. coli* ML-35 strain lacks lactose permease activity but produces β-galactosidase constitutively in the cytosol [25]. A derivative *E. coli* ML-35p harboring pBR322 produces β-lactamase in the periplasmic space [26]. *E. coli* ML-35 or *E. coli* ML-35p cells at mid-logarithmic growth phase were resuspended in 5 mM HEPES buffer (pH 7.2) at approximately 10^8 cells/mL and treated with different concentrations of endolysins from 0 to 1.28 μM. The OM and inner membrane (IM) permeability was determined via colorimetric assays using chromogenic substrates nitrocefin (Abcam) and *o*-nitrophenyl-β-D-galactopyranoside (ONPG; KisanBio, Seoul, Korea), respectively. The cell suspension was supplemented with nitrocefin at 50 μg/mL or ONPG at 1.5 mM, and the chromogenic changes were measured at 486 nm (nitrocefin) and 420 nm (ONPG), respectively, using a Synergy HTX microplate reader.

2.12. Western blot analysis

E. coli cells at approximately 10^8 cells/mL were treated with 0.32 μM endolysins in 5 mM HEPES buffer (pH 7.2) and were centrifuged at 10,000 ×*g* for 5 min to separate the endolysin-bound bacterial cells (bacterial pellet: P) from unbound endolysin molecules (supernatant solution: S). Bacterial cells were washed, resuspended in 20 mM Tris-HCl (pH 7.5) buffer, and then disrupted using sonication. The cytosolic fraction (bacterial cytosol: C) was separated from insoluble macromolecules containing the membranous fraction (M) using ultracentrifugation (100,000 ×*g* for 1 h). The C fraction was concentrated using trichloroacetic acid (TCA) precipitation and a quantity of protein equal to 10 μg was mixed with 4× Laemmli buffer (Bio-Rad) at a 3:1 ratio. For the P fraction, bacterial cells equivalent to 10^7 cells were resuspended directly in 1× Laemmli buffer (Bio-Rad). Likewise, the insoluble cell debris derived from 10^7 cells was dissolved in 1× Laemmli buffer and used as the M fraction. The S fraction was also concentrated using TCA and an aliquot derived from 10^7 cells was mixed with 2× Laemmli buffer (Bio-Rad) at a 1:1 ratio. Proteins were separated via SDS-PAGE using 12 % polyacrylamide gels and transferred to a

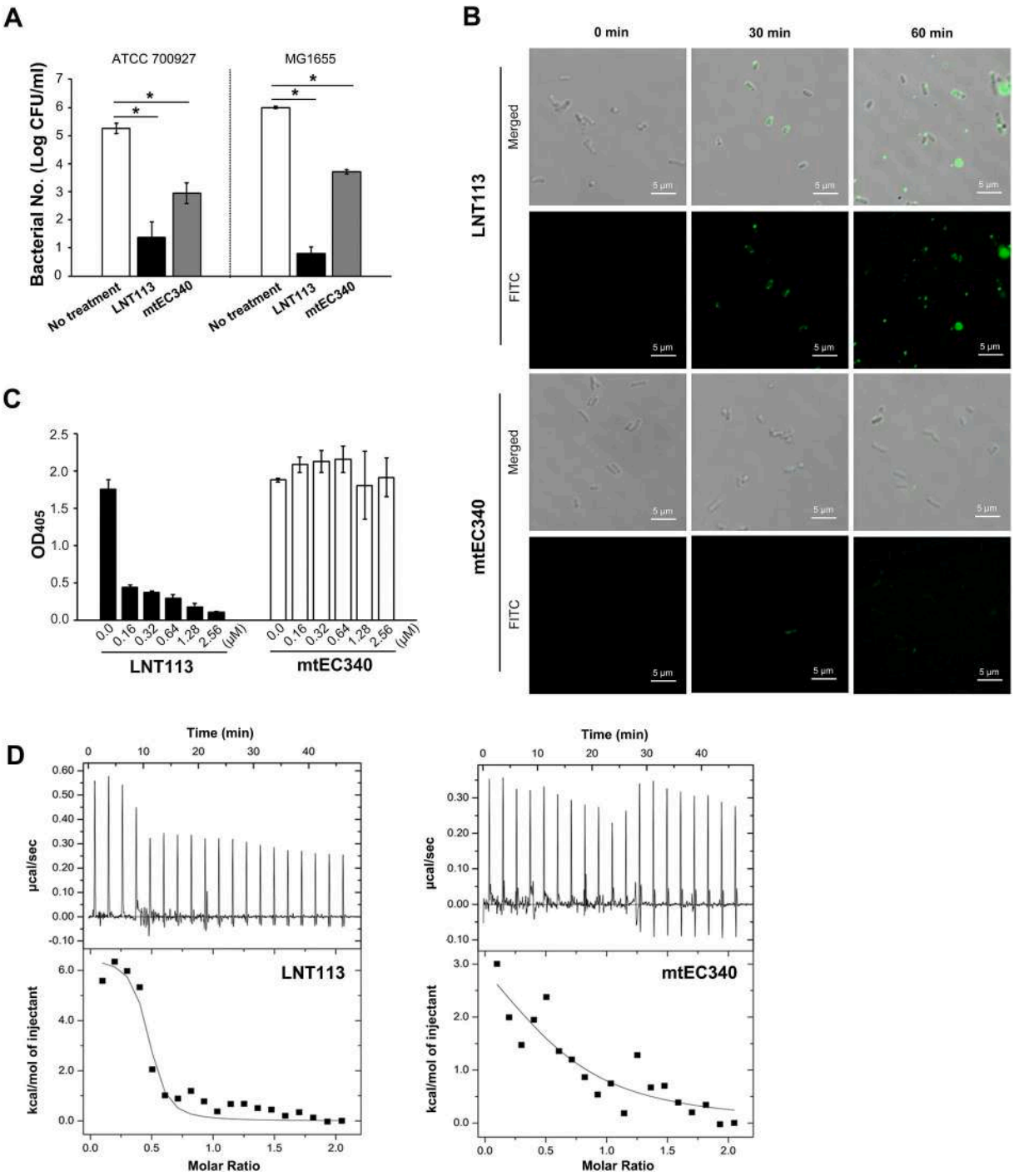

Fig. 1. Cecropin A fusion increased the binding affinity with lipopolysaccharide (LPS)
(A) Viability of *Escherichia coli* O157:H7 ATCC 700927 and MG1655 after LNT113 or mtEC340 treatment. Bacterial cells resuspended in 20 mM Tris-HCl (pH 7.5) were treated with endolysins at 2 μM for 2 h. Asterisk indicates a significant difference compared with no treatment (P value <0.05). (B) Localization of LNT113 and mtEC340. *E. coli* cells resuspended in PBS were treated with FITC-labeled endolysins at 5 μM for 30 min and observed using a confocal microscope. (C) Comparison of LPS neutralization ability between LNT113 and mtEC340. *E. coli* LPS molecules were treated with endolysins at different concentrations for 1 h, and the unbound LPS was estimated by measuring 4-nitroaniline at 405 nm. (D) Thermodynamics of binding between LNT113 and LPS. The upper panels display the raw data of heat changes of endolysins following the time-coursed injections of LPS, and the lower panels display the processed curves obtained by titration of LPS (500 μM) with each endolysin (50 μM).

polyvinylidene difluoride (PVDF) membrane (Bio-Rad). The membrane was blocked in 5 % skimmed milk solution. LNT113 and mtEC340, containing C-terminal His_6 tag, and DnaK were identified using anti-His (1:10,000 dilution; Invitrogen) and anti-DnaK (1:10,000 dilution; Enzo Life Sciences, Farmingdale, NY, USA) primary antibodies, respectively, along with anti-mouse IgG horseradish peroxidase-conjugated secondary antibody (1:5000 dilution; Bio-Rad). The PVDF membrane was processed using Amersham ECL detection reagents (Cytiva, Seoul, Korea), and the proteins were identified using a ChemiDoc MP imaging system (Bio-Rad).

Table 1
Minimum inhibitory concentrations of LNT113 and mtEC340 against *Escherichia coli* strains.

Bacterial strain	LNT113		mtEC340	
	μg/mL	μM	μg/mL	μM
Escherichia coli ATCC 8739	8	0.35	> 128	> 7.02
E. coli ATCC 25922	32	1.38	> 128	> 7.02
E. coli FORC81	8	0.35	> 128	> 7.02
E. coli F-485	4	0.17	> 128	> 7.02
E. coli F-524	8	0.35	> 128	> 7.02
E. coli F-576	4	0.17	> 128	> 7.02

2.13. Statistical analysis

All assays and quantitative measurements were conducted at least three times using multiple biological replicates to ensure experimental results. Statistical analysis was performed using GraphPad Prism 5 (GraphPad Software Inc., San Diego, CA, USA). All values are expressed as the mean ± standard deviation. Student's *t*-test was employed, and statistical significance was set at a P value < 0.05.

3. Results

3.1. Cecropin A fusion increases the interaction with bacterial LPS

EC340, an endolysin containing a phage-related lysozyme (muramidase) domain, was mutated to mtEC340 through the substitution of seven amino acids and further fused with cecropin A at its N-terminus to generate LNT113, which is a 223-amino-acid protein with a molecular mass of 23.17 kDa [14] (Supplementary Fig. 1). LNT113 more efficiently reduced the number of viable *E. coli* cells than did mtEC340 (Fig. 1A). The enhanced bacteriolytic activity imparted by cecropin A fusion was also observed in the turbidity reduction assay (Supplementary Fig. 2) and the MIC measurements (Table 1). Notably, LNT113 could also inactivate a colistin-resistant strain, *E. coli* FORC81, suggesting that LNT113 exerted a different mechanism of action from that of colistin. When the interaction between endolysins and *E. coli* was monitored, LNT113 located and lysed bacterial cells within 60 min, but mtEC340 could hardly locate the cells in the same duration (Fig. 1B).

We examined whether cecropin A fusion increased the neutralization ability of mtEC340 with LPS (Fig. 1C). LPS was incubated with mtEC340 or LNT113, and the level of unbound LPS was estimated using LAL-based assay. Even at 0.16 μM, LNT113 neutralized LPS and prevented LPS-

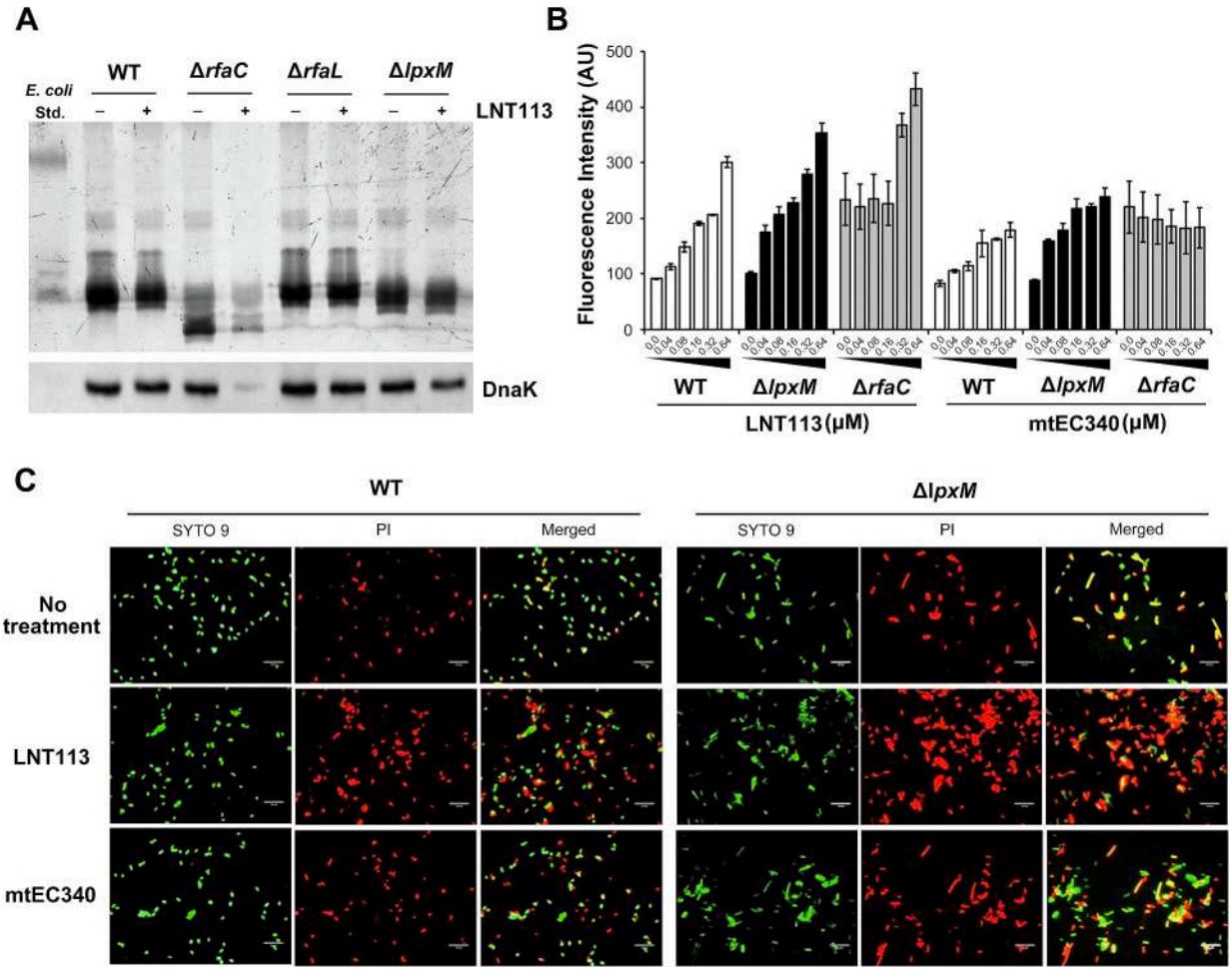

Fig. 2. Stability of the core oligosaccharide and lipid A affected the bactericidal activity of LNT113
(A) Comparison of lipopolysaccharides (LPSs) between *Escherichia coli* MG1655 (WT) and its LPS mutants (Δ*rfaC*, Δ*rfaL*, and Δ*lpxM*) after LNT113 treatment. Bacterial cells were treated with LNT113 at 0.64 μM for 1 h and LPSs were extracted and analyzed. DnaK was used to normalize the total cells between lanes. (B) Comparison of membranous disruption between WT and LPS mutants after LNT113 treatment. Bacterial cells were incubated with different concentrations of endolysins for 1 h, and the fluorescence intensity was measured after PI staining. (C) Microscopic observation of WT and Δ*lpxM* strains after endolysin treatment. Bacterial cells were treated with 0.02 μM edolysins for 30 min, stained using SYTO 9 (live or dead) and PI (dead) for 5 min, and analyzed via fluorescence microscopy. Scale bar is 10 μm.

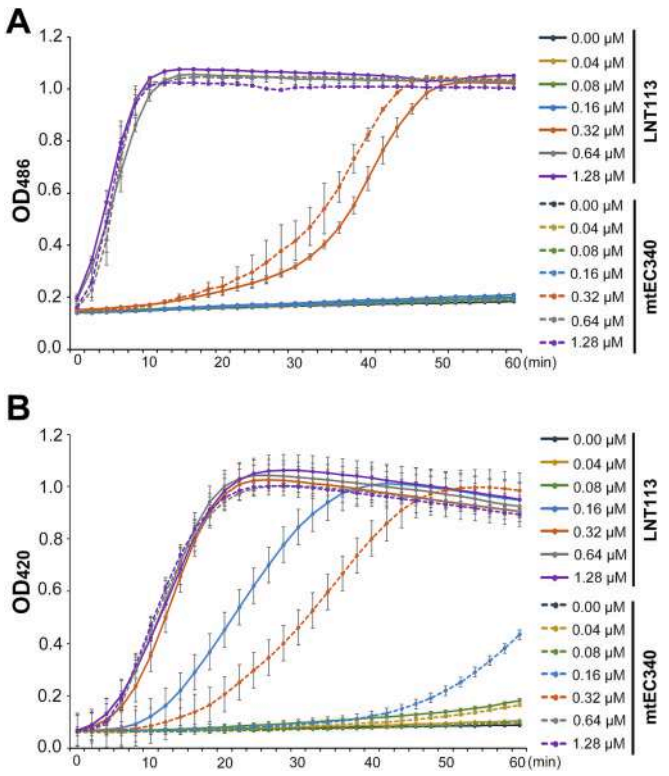

Fig. 3. Cecropin A fusion accelerated the disruption of the inner membrane (IM)

(A) Disruption of the outer membrane (OM) of *Escherichia coli* ML-35p cells after endolysin treatment. Bacterial cells were treated with different concentrations of LNT113 (solid line) and mtEC340 (dotted line), and OM permeability was determined via colorimetric change of nitrocefin by periplasmic β-lactamase at 486 nm for 1 h. (B) Disruption of the inner membrane (IM) of *E. coli* ML-35p cells after endolysin treatment. Bacterial cells were treated with different concentrations of LNT113 (solid line) and mtEC340 (dotted line), and IM permeability was determined via colorimetric change of *o*-nitrophenyl-β-D-galactopyranoside by cytoplasmic β-galactosidase at 420 nm for 1 h.

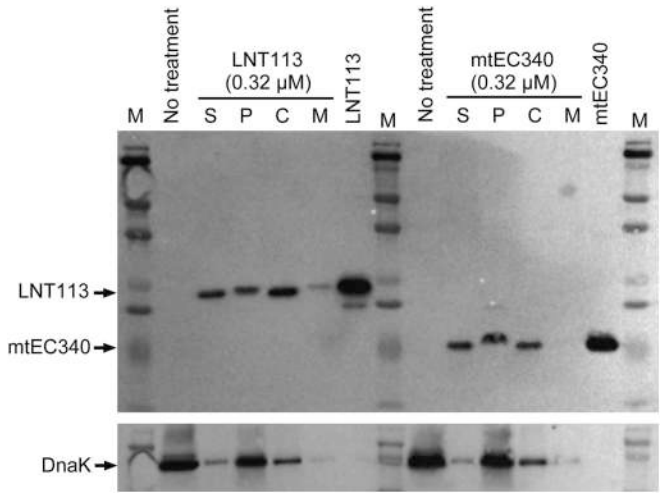

Fig. 4. Localization of intracellular LNT113 and mtEC340 after *Escherichia coli* treatment

E. coli MG1655 cells were treated with endolysins at 0.32 μM and centrifuged to separate the endolysin-bound bacterial cells (bacterial pellet: P) from unbound endolysin molecules (supernatant solution: S). Using sonication, P fractions were physically disrupted and subjected to ultracentrifugation to separate the cytosolic fraction (bacterial cytosol: C) from insoluble macromolecules containing the membranous fraction (M). Endolysins containing C-terminal His_6 tag were identified using anti-His antibody. DnaK levels were compared in parallel to normalize the cell amounts.

mediated release of LAL end-product 4-nitroaniline. However, mtEC340 did not alter the ability of LPS to stimulate LAL coagulation, indicating its low affinity to LPS at the used concentrations. The binding affinity with LPS was also compared between LNT113 and mtEC340 using ITC (Fig. 1D). Both endolysins demonstrated endothermic reactions with LPS. The binding affinity of LNT113 to LPS was approximately 34-fold greater than that of mtEC340 to LPS; K_D values of LNT113 and mtEC340 were estimated at 3.5×10^{-7} M and 1.2×10^{-5} M, respectively. The thermodynamic parameters of interaction between endolysins and LPS are summarized in Supplementary Table 3. These results suggest that cecropin A fused to mtEC340 increased the affinity with LPS, thereby facilitating the access of LNT113 to the bacterial envelope.

3.2. Integrity of core oligosaccharide and lipid A is critical for LNT113 activity

To explore which LPS structural components are crucial for the bactericidal activity of LNT113, *E. coli* strains defective in LPS structures, i.e., Δ*rfaC*, Δ*rfaL*, and Δ*lpxM*, were treated with endolysins (Fig. 2). LPS profiles of Δ*rfaL* and Δ*lpxM* were comparable to that of a wild-type strain while Δ*rfaC* mutant strain was defective in the core moiety (Supplementary Fig. 3). LNT113 treatment did not cause structural alterations of LPS in any bacterial strain (Fig. 2A), which ruled out the possibility of LPS disruption by LNT113. The Δ*rfaC* mutant strain was attenuated in the growth (Supplementary Fig. 4) and was more likely to be lysed by LNT113, implying that deletion of *rfaC* might destabilize the membrane structure. After applying varied concentrations of endolysins to *E. coli* cells, the membrane integrity was analyzed via PI staining, which only penetrates compromised bacterial membranes and stains cytosolic DNA and RNA [27]. Compared to mtEC340, LNT113 accelerated the membrane destruction of wild-type bacteria. Both endolysins impaired bacterial membranes more efficiently in the Δ*lpxM* mutant, indicating that the lipid A layer integrity was important in obstructing the penetration of either endolysin (Fig. 2B). The increased susceptibility of the Δ*lpxM* mutant to both endolysins was validated in a microscopic analysis (Fig. 2C). The Δ*rfaC* strain was vulnerable to PI staining even without endolysin treatment. However, neither endolysin was able to further disrupt the membrane where the core oligosaccharide was defective (Fig. 2B). LNT113, only at a higher concentration (≥0.32 μM), caused additional membrane destabilization in the Δ*rfaC* strain. This finding suggests that both LNT113 and mtEC340 depend on the core oligosaccharide moiety to interact with the bacterial membrane. N-terminal cecropin A may help LNT113 circumvent the restricted accessibility in the Δ*rfaC* strain by interacting with the two phosphate groups of D-glucosamine disaccharide in the lipid A layer and the hydrophobic lipid A anchor.

3.3. Cecropin A fusion increased the permeability across the IM

Cecropins with amphipathic and hydrophobic helical structures are intrinsically capable of destabilizing various types of lipid bilayers with negatively-charged headgroups and hydrophobic acyl chains. To address whether cecropin A fusion facilitated the destabilization of both the OM and IM, the permeability of the two membranes was individually evaluated following mtEC340 and LNT113 treatments. *E. coli* ML-35 is defective in lactose permeability but constitutively produces cytosolic β-galactosidase [25]. *E. coli* ML-35p, a derivative transformed with pBR322, produces a plasmid-encoded periplasmic β-lactamase [26]. *E. coli* ML-35p cells producing periplasmic β-lactamase were treated with endolysins, and the OM disruption was estimated via hydrolysis of chromogenic β-lactam (Fig. 3A). Both types of endolysins could destabilize the OM at 0.32 μM or more. Interestingly, the OM permeability was comparable between mtEC340 and LNT113 treatments. Further, the

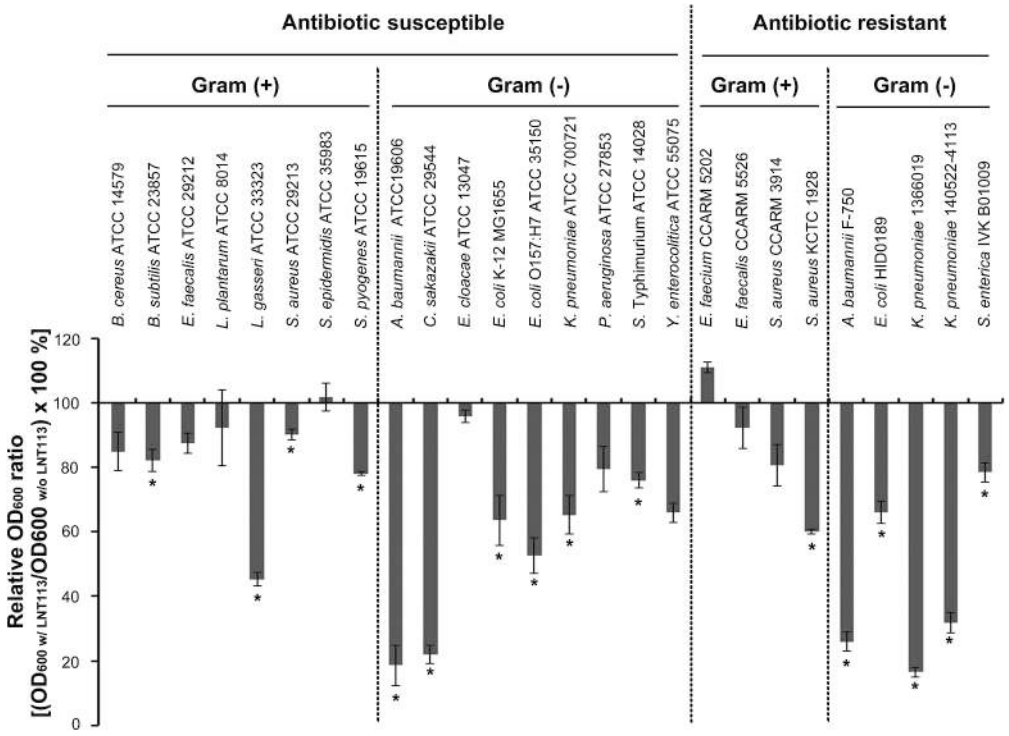

Fig. 5. Killing activity of LNT113 against Gram-positive and -negative bacteria
Cells of different bacterial strains at the log growth phase were resuspended in 20 mM Tris-HCl (pH 7.5) and treated with LNT113 at 0.64 μM for 1 h. Optical densities in the presence and absence of LNT113 were measured at 600 nm and used to estimate the turbidity reduction. Asterisk indicates a significant difference compared with no treatment (P value <0.05). Bacterial strains with antibiotic resistance are as follows: *Enterococcus faecium* CCARM 5202 against ampicillin, erythromycin, gentamicin, and norfloxacin; *Enterococcus faecalis* CCARM 5526 against gentamicin and streptomycin; *Staphylococcus aureus* CCARM 3914 against ciprofloxacin, clindamycin, erythromycin, gentamicin, norfloxacin, oxacillin, penicillin, trimethoprim-sulfamethoxazole, and tetracycline; *S. aureus* KCTC 1928 against methicillin; *A. baumannii* F-750 against carbapenem; *Escherichia coli* HID0189 against tetracyclin; *Klebsiella pneumoniae* 1366019 against carbapenem; *K. pneumoniae* 140522-4113 against carbapenem; *Salmonella enterica* IVK B01009 against tetracycline.

permeability of bacterial IM was assessed in *E. coli* ML-35 cells producing cytoplasmic β-galactosidase. Compared to mtEC340 treatment, LNT113 treatment resulted in a more pronounced hydrolysis of the chromogenic substrate ONPG (Fig. 3B). Considering that cecropin A fusion improved the binding affinity of LNT113 with LPS, it is plausible to expect that LNT113 exerts more permeability through the OM than mtEC340. However, this finding showed that cecropin A fusion was more likely to facilitate the destabilization of the IM.

To localize the internalized endolysins, *E. coli* cells were treated with mtEC340 and LNT113, and bacterial membranous fractions were separated from the cytoplasmic contents (Fig. 4). The levels of protein co-precipitated with bacterial cells were comparable between mtEC340 and LNT113. However, LNT113 was internalized into the cytosol and membranes more profoundly than mtEC340. This phenomenon might be attributable to cecropin A, which increased the binding affinity with LPS and the permeability across the IM.

The accelerated IM destabilization due to cecropin A fusion encouraged us to test the bactericidal activity of LNT113 against diverse bacterial species including Gram-positive bacteria (Fig. 5). LNT113 treatment reduced the optical density of bacterial suspensions of many different Gram-negative pathogens, including *Acinetobacter baumannii*, *Cronobacter sakazakii*, *Klebsiella pneumoniae*, *Salmonella* spp., and *Yersinia enterocolitica*. Interestingly, some Gram-positive bacterial species, such as *Bacillus subtilis*, *Lactobacillus gasseri*, *Staphylococcus aureus*, and *Streptococcus pyogenes* were also degraded by LNT113.

4. Discussion

Natural endolysins have significant limitations in their use as alternative antibacterial agents against Gram-negative infections, because they are generally unable to penetrate the OM and reach the underlying peptidoglycans. However, some exceptional endolysins with intrinsic lytic activity against Gram-negative bacteria typically have a globular structure and possess a cationic or amphipathic domain, which presumably helps in docking the negatively-charged LPS and facilitating penetration into the OM [10,12]. The crystal structure of mtEC340 was predicted to have a globular conformation consisting of 8 α-helices and 2 loops in solution, with a positive overall surface charge [28]. These structural features may be favorable for mtEC340 to interact with and penetrate bacterial OM. Typical cecropin family peptides form helix-hinge-helix structures in contact with membrane-mimetic structures [29]. Their N-terminal amphipathic α-helix with positively-charged amino acids' side chains outwards is predicted to induce electrostatic interactions with the negatively-charged region of LPS, such as the core oligosaccharide and lipid A, while their C-terminal hydrophobic α-helix can intercalate between the hydrophobic acyl chains in the lipid A layer [30,31]. Thus, cecropin A at the N-terminus of LNT113 is speculated to bind to the negatively-charged moiety of LPS and wedge into the tightly packed lipid A molecules through hydrophobicity-driven association. Colistin with polycationic and hydrophobic moieties is also known to interact with the negatively-charged phosphate groups of LPS and penetrate the outer leaflet of the OM [32]. However, LNT113 inactivated a colistin-resistant *E. coli* strain, indicating a different mechanism of LNT113 from that of colistin. The superior lytic activity of LNT113 to that of cecropin A alone was also observed in the previous study [14]. Despite the increased interaction of LNT113 with LPS, cecropin A fusion did not increase OM permeability, although it accelerated IM destabilization. The tight interaction between cecropin A and LPS may have impeded the passage of cecropin A-fused proteins. Sugars and phosphate groups within the core oligosaccharide layer are presumed to present a

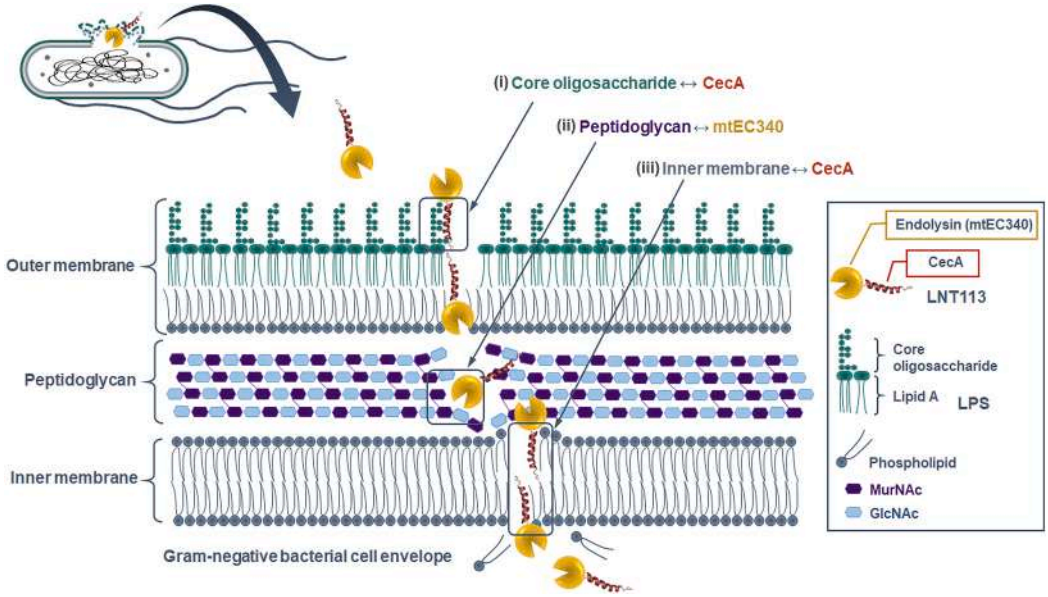

Fig. 6. Presumed mechanism of action of LNT113 against Gram-negative bacteria
The mode of triple action of LNT113 was suggested: (i) facilitated targeting of lipopolysaccharides by the interaction between core oligosaccharide and cecropin A, (ii) lysis of peptidoglycans by the muramidase activity of mtEC340 moiety, and (iii) destabilization of the inner membrane by the interaction with cecropin A.

kinetic barrier to cecropin A penetration, and the compromised core oligosaccharide lacking sugars and phosphates hastened the passage of cecropin A [22]. The threshold surface concentration model has been proposed to understand the bacteriolytic activity of antimicrobial peptides [33,34]: drugs at low concentrations are accumulated at the lipid A outer leaflet of the OM. However, they can induce abrupt and localized permeabilization in the OM once a threshold concentration is achieved. We observed that LNT113 at low concentrations (<0.32 μM) failed to disrupt the membranes defective in the core oligosaccharide but abruptly caused bacterial lysis at a higher concentration. The core oligosaccharide layer can provide negatively-charged phosphate groups for electrostatic interactions with cecropin A but is also hypothesized to act as a kinetic barrier, detaining and preventing cecropin A from penetrating the lipid A layer [22]. Given the lack of an intensive interaction with and a kinetic barrier against cecropin A in the Δ*rfaC* strain, LNT113 may need a higher threshold concentration for its passage. mtEC340 lacking cecropin A failed to degrade the Δ*rfaC* membranes even at higher concentrations, indicating cecropin A-mediated membrane degradation of LNT113 in the Δ*rfaC* strain. Once the OM is permeabilized by cecropin A, IM permeabilization occurs subsequently [22]. Besides the interaction with the core oligosaccharide, the integrity of lipid A, especially of its hydrophobic acyl chains, was critical to resist the accessibility of exogenous endolysins, independent of cecropin A fusion. Despite the crucial roles of core oligosaccharide and lipid A in the action of LNT113, the molecular details that govern the interaction between LNT113 and LPS remain undefined. In silico docking model with different LPS structures may provide a blueprint on how LNT113 penetrates the OM and reach the underlying peptidoglycans.

It is speculative that the superior lytic activity of LNT113 was attributable to the mode of triple action: (i) facilitated targeting of LPS by cecropin A, (ii) lysis of peptidoglycans by mtEC340 moiety, and (iii) accelerated IM disruption by cecropin A (Fig. 6). Engineering endolysins using cecropin A can be a prospective strategy to completely destabilize the layered bacterial envelope architecture. Furthermore, co-administration with cecropin-fused endolysins can help in the permeation of other bacteriostatic antimicrobials that inhibit protein synthesis or DNA replication but are ineffective in Gram-negative pathogens owing to their structural barrier, the OM.

5. Conclusions

This study aimed to explore the mechanism of lytic activity in cecropin A-fused endolysin, LNT113. Cecropin A fusion facilitated the interaction of LNT113 with LPS as well as IM destabilization. Therefore, LNT113 could not only degrade its intrinsic target peptidoglycan layers but also impair bacterial membranes, demonstrating outstanding lytic activity against Gram-negative bacteria. Engineering endolysins using cecropins has a potential to overcome the limitation of applying intrinsic endolysins to Gram-negative pathogens.

CRediT authorship contribution statement

Jeongik Cho: Methodology, Investigation, Data curation. **Hye-Won Hong:** Methodology, Investigation, Data curation. **Kyungah Park:** Methodology, Data curation. **Heejoon Myung:** Resources, Conceptualization. **Hyunjin Yoon:** Writing – review & editing, Writing – original draft, Supervision, Resources, Conceptualization.

Declaration of competing interest

Heejoon Myung, Hye-Won Hong has patent issued to None. None.

Data availability

Data will be made available on request.

Acknowledgements

This work was supported by the Korea Health Industry Development Institute [KHIDI, grant number HI21C2447], funded by the Ministry of Health & Welfare, as well as the Bio & Medical Technology Development Program from the National Research Foundation of Korea [NRF, grant number 2021M3A9I4026029], funded by the Ministry of Science & ICT. The funders had no role in the design of the study and the interpretation of data.

Ethical approval

Not required.

Sequence information

None.

Appendix A. Supplementary data

Supplementary data to this article can be found online at https://doi.org/10.1016/j.ijbiomac.2024.129493.

References

[1] G. Dubourg, J.C. Lagier, C. Robert, F. Armougom, P. Hugon, S. Metidji, N. Dione, N. P. Dangui, A. Pfleiderer, J. Abrahao, D. Musso, L. Papazian, P. Brouqui, F. Bibi, M. Yasir, B. Vialettes, D. Raoult, Culturomics and pyrosequencing evidence of the reduction in gut microbiota diversity in patients with broad-spectrum antibiotics, Int. J. Antimicrob. Agents 44 (2) (2014) 117–124.

[2] F. Abdelrahman, M. Easwaran, O.I. Daramola, S. Ragab, S. Lynch, T.J. Oduselu, F. M. Khan, A. Ayobami, F. Adnan, E. Torrents, S. Sanmukh, A. El-Shibiny, Phage-encoded endolysins, Antibiotics (Basel) 10 (2) (2021).

[3] K. Abdelkader, H. Gerstmans, A. Saafan, T. Dishisha, Y. Briers, The preclinical and clinical progress of bacteriophages and their lytic enzymes: the parts are easier than the whole, Viruses 11 (2) (2019).

[4] Y. Briers, G. Volckaert, A. Cornelissen, S. Lagaert, C.W. Michiels, K. Hertveldt, R. Lavigne, Muralytic activity and modular structure of the endolysins of Pseudomonas aeruginosa bacteriophages phiKZ and EL, Mol. Microbiol. 65 (5) (2007) 1334–1344.

[5] X. Cheng, X. Zhang, J.W. Pflugrath, F.W. Studier, The structure of bacteriophage T7 lysozyme, a zinc amidase and an inhibitor of T7 RNA polymerase, Proc. Natl. Acad. Sci. U. S. A. 91 (9) (1994) 4034–4038.

[6] M.J. Loessner, K. Kramer, F. Ebel, S. Scherer, C-terminal domains of listeria monocytogenes bacteriophage murein hydrolases determine specific recognition and high-affinity binding to bacterial cell wall carbohydrates, Mol. Microbiol. 44 (2) (2002) 335–349.

[7] M. Schmelcher, D.M. Donovan, M.J. Loessner, Bacteriophage endolysins as novel antimicrobials, Future Microbiol. 7 (10) (2012) 1147–1171.

[8] M.J. Love, G.S. Abeysekera, A.C. Muscroft-Taylor, C. Billington, R.C.J. Dobson, On the catalytic mechanism of bacteriophage endolysins: opportunities for engineering, Biochim. Biophys. Acta, Proteins Proteomics 1868 (1) (2020) 140302.

[9] X. Wang, L. Han, J. Rong, H. Ren, W. Liu, C. Zhang, Endolysins of bacteriophage vB_Sal-S-S10 can naturally lyse Salmonella enteritidis, BMC Vet. Res. 18 (1) (2022) 410.

[10] W.C.B. Lai, X. Chen, M.K.Y. Ho, J. Xia, S.S.Y. Leung, Bacteriophage-derived endolysins to target gram-negative bacteria, Int. J. Pharm. 589 (2020) 119833.

[11] Y. Larpin, F. Oechslin, P. Moreillon, G. Resch, J.M. Entenza, S. Mancini, In vitro characterization of PlyE146, a novel phage lysin that targets Gram-negative bacteria, PLoS One 13 (2) (2018) e0192507.

[12] N.N. Sykilinda, A.Y. Nikolaeva, M.M. Shneider, D.V. Mishkin, A.A. Patutin, V. O. Popov, K.M. Boyko, N.L. Klyachko, K.A. Miroshnikov, Structure of an Acinetobacter broad-range prophage endolysin reveals a C-terminal alpha-Helix with the proposed role in activity against live bacterial cells, Viruses 10 (6) (2018).

[13] Y. Briers, M. Walmagh, V. Van Puyenbroeck, A. Cornelissen, W. Cenens, A. Aertsen, H. Oliveira, J. Azeredo, G. Verween, J.P. Pirnay, S. Miller, G. Volckaert, R. Lavigne, Engineered endolysin-based "Artilysins" to combat multidrug-resistant gram-negative pathogens, mBio 5 (4) (2014) e01379-14.

[14] H.W. Hong, Y.D. Kim, J. Jang, M.S. Kim, M. Song, H. Myung, Combination effect of engineered Endolysin EC340 with antibiotics, Front. Microbiol. 13 (2022) 821936.

[15] T.A. Holak, A. Engstrom, P.J. Kraulis, G. Lindeberg, H. Bennich, T.A. Jones, A. M. Gronenborn, G.M. Clore, The solution conformation of the antibacterial peptide cecropin A: a nuclear magnetic resonance and dynamical simulated annealing study, Biochemistry 27 (20) (1988) 7620–7629.

[16] H. Steiner, D. Andreu, R.B. Merrifield, Binding and action of cecropin and cecropin analogues: antibacterial peptides from insects, Biochim. Biophys. Acta 939 (2) (1988) 260–266.

[17] L. Silvestro, J.N. Weiser, P.H. Axelsen, Antibacterial and antimembrane activities of cecropin a in Escherichia coli, Antimicrob. Agents Chemother. 44 (3) (2000) 602–607.

[18] Z. Oren, Y. Shai, Mode of action of linear amphipathic alpha-helical antimicrobial peptides, Biopolymers 47 (6) (1998) 451–463.

[19] K.A. Datsenko, B.L. Wanner, One-step inactivation of chromosomal genes in Escherichia coli K-12 using PCR products, Proc. Natl. Acad. Sci. U. S. A. 97 (12) (2000) 6640–6645.

[20] D. Liu, P.R. Reeves, Escherichia coli K12 regains its O antigen, Microbiology (Reading) 140 (Pt 1) (1994) 49–57.

[21] M.A. Jorgenson, K.D. Young, Interrupting biosynthesis of O antigen or the lipopolysaccharide core produces morphological defects in Escherichia coli by sequestering Undecaprenyl phosphate, J. Bacteriol. 198 (22) (2016) 3070–3079.

[22] A. Agrawal, J.C. Weisshaar, Effects of alterations of the E. coli lipopolysaccharide layer on membrane permeabilization events induced by Cecropin A, Biochim. Biophys. Acta Biomembr. 1860 (7) (2018) 1470–1479.

[23] H. Xu, J. Ling, Q. Gao, H. He, X. Mu, Z. Yan, S. Gao, X. Liu, Role of the lpxM lipid A biosynthesis pathway gene in pathogenicity of avian pathogenic Escherichia coli strain E058 in a chicken infection model, Vet. Microbiol. 166 (3–4) (2013) 516–526.

[24] S. Rezania, N. Amirmozaffari, B. Tabarraei, M. Jeddi-Tehrani, O. Zarei, R. Alizadeh, F. Masjedian, A.H. Zarnani, Extraction, purification and characterization of lipopolysaccharide from Escherichia coli and Salmonella typhi, Avicenna J. Med. Biotechnol. 3 (1) (2011) 3–9.

[25] R.I. Lehrer, A. Barton, K.A. Daher, S.S. Harwig, T. Ganz, M.E. Selsted, Interaction of human defensins with Escherichia coli. Mechanism of bactericidal activity, J. Clin. Invest. 84 (2) (1989) 553–561.

[26] R.I. Lehrer, A. Barton, T. Ganz, Concurrent assessment of inner and outer membrane permeabilization and bacteriolysis in E. coli by multiple-wavelength spectrophotometry, J. Immunol. Methods 108 (1–2) (1988) 153–158.

[27] L. Boulos, M. Prevost, B. Barbeau, J. Coallier, R. Desjardins, LIVE/DEAD BacLight: application of a new rapid staining method for direct enumeration of viable and total bacteria in drinking water, J. Microbiol. Methods 37 (1) (1999) 77–86.

[28] J.M. Wang, S.H. Seok, W.S. Yoon, J.H. Kim, M.D. Seo, Crystal structure of the engineered endolysin mtEC340M, Acta Crystallogr. F Struct. Biol. Commun. 79 (Pt 5) (2023) 105–110.

[29] A.M. Cole, R.O. Darouiche, D. Legarda, N. Connell, G. Diamond, Characterization of a fish antimicrobial peptide: gene expression, subcellular localization, and spectrum of activity, Antimicrob. Agents Chemother. 44 (8) (2000) 2039–2045.

[30] H.L. Chu, Y.H. Chih, K.L. Peng, C.L. Wu, H.Y. Yu, D. Cheng, Y.T. Chou, J.W. Cheng, Antimicrobial peptides with enhanced salt resistance and antiendotoxin properties, Int. J. Mol. Sci. 21 (18) (2020).

[31] E. Lee, K.W. Jeong, J. Lee, A. Shin, J.K. Kim, J. Lee, D.G. Lee, Y. Kim, Structure-activity relationships of cecropin-like peptides and their interactions with phospholipid membrane, BMB Rep. 46 (5) (2013) 282–287.

[32] F.F. Andrade, D. Silva, A. Rodrigues, C. Pina-Vaz, Colistin update on its mechanism of action and resistance, present and future challenges, Microorganisms 8 (11) (2020).

[33] N. Rangarajan, S. Bakshi, J.C. Weisshaar, Localized permeabilization of E. coli membranes by the antimicrobial peptide Cecropin A, Biochemistry 52 (38) (2013) 6584–6594.

[34] C.G. Starr, J. He, W.C. Wimley, Host cell interactions are a significant barrier to the clinical utility of peptide antibiotics, ACS Chem. Biol. 11 (12) (2016) 3391–3399.